Int. J. of Geosynth. and Ground Eng. (2015) 1:6
DOI 10.1007/s40891-014-0008-9

ORIGINAL PAPER

Influence of Particle Size on the Friction and Interfacial Shear Strength of Sands of Similar Morphology

Prashanth Vangla · Gali Madhavi Latha

Received: 8 December 2014 / Accepted: 27 December 2014 / Published online: 15 January 2015

Abstract Size and morphological characteristics of particles play vital role on the shear and interfacial shear strength of sands. Often, effects of these parameters are merged and cannot be easily separated. Effect of size of the particles on the shear and interfacial shear strength of sands is presented in this paper through direct shear and interface direct shear tests complemented with image analyses and surface roughness studies. To eliminate the effect of morphological characteristics, three sands of different particle sizes with similar morphological characteristics like angularity, roundness, sphericity and roughness were selected for the study. These morphological characteristics for all three sands were determined from the analysis of scanning electron microscope images and were found to be similar for all three sands. It was observed from the symmetric direct shear tests that the particle size has no effect on the peak friction angle when the tests were carried out at same void ratio. However, ultimate friction angles were affected by the particle size. Shear band thickness was estimated from image segmentation analysis of the profiles of colored sand columns during shear and the same was correlated to the particle size. Interface direct shear tests were carried out on sand–geomembrane interfaces to study the effect of particle size on the interfacial shear strength. Microscopic images of geomembranes were captured after the interface shear tests to understand the change in surface roughness of the geomembrane due to particle indentations. Surface roughness studies on geomembrane samples after the tests confirmed that the plowing and groove formation on geomembranes during interface shear tests depend on the particle size as well as the relative roughness of the sand particles with respect to the membrane. Sand of medium particle size showed highest interfacial strength because of more number of effective contacts per unit area of the interface.

Keywords Particle size · Morphology · Geomembrane · Image analysis · Surface roughness · Symmetric loading direct shear tests

P. Vangla · G. M. Latha (✉)
Civil Engineering Department, Indian Institute of Science, Bangalore 5600012, India
e-mail: madhavi@civil.iisc.ernet.in

P. Vangla
e-mail: pvangla@civil.iisc.ernet.in

Introduction

The stress–strain response and volume change behavior of sands in shear and interface shear are mainly influenced by the normal stress, method of testing and testing materials [1–6], morphological characteristics of sand [7–12] and surface roughness of the geosynthetic material at the interface [13–18]. Morphological characteristics of sand grains reflect the formation process, transportation process and material composition. These characteristics include angularity, roundness, sphericity, regularity and roughness. Several studies are available in literature that correlate the morphological characteristics of sand grains to the shear strength. Through systematic analysis of microphotographs of sand grains and oedometer tests, Cho et al. [8] observed that the increase in angularity of grains leads to increase in constant volume critical state friction angle and recommended that particle shape should be characterized and should be included in the classifications, especially for gravels and sands. Lim et al. [19] showed that particle shape and size have significant influence on the engineering properties of sands. Sand of different origins having

wide range of particle size and morphological characteristics were studied through direct shear tests and image analysis and it was observed that the peak and ultimate friction angles as well as dilatancy were significantly affected by the particle shape and gradation of the sands. Santamarina and Cascante [20] studied the effect of particle roughness on the wave propagation through resonant column tests and observed that the surface roughness decreases contact stiffness and increases the interparticle friction.

Importance of understanding the interface shear behavior of sand with geosynthetics arises from the need for effective design of geotechnical structures like geosynthetic liners, retaining walls and embankments. Shear and bond stiffness at the interface depend on the properties of the soil and the geosynthetic material as well as the bonding characteristics of these materials. Many studies were reported on the influence of particle size and morphology on the shear behavior of sand–geomembrane interfaces. Fuggle [21] studied the effects of size and gradation of sand particles on the shear behavior of sand–geomembrane interfaces and observed that the large displacement friction angles and dilation angles were affected significantly by the particle size and gradation. Williams and Houlihan [13] showed that surface roughness, particle size, type and composition and the water content are the major parameters that can influence the interface shear behavior of soil-geomembrane. Similar other studies were reported on the effect of particle size [14], surface hardness of the polymer [15], surface roughness [16], and normal stress [17] on the interface shear behavior of sands. There are many studies in which the particle morphology and classifications were done by the image based technologies [22–24]. The recent advancements in digital image technology provides an accurate estimation of the size and shape characteristics compared to conventional measurement techniques. Hence the present study adopts image analysis for characterizing the grain size and morphology, shear band thickness and surface roughness as well.

Though the effect of particle size on the shear strength behavior is studied well by earlier researchers, the effects of particle size and morphology are often combined and the individual effect of these parameters cannot be easily separated. Independent effect of particle size devoid of effects due to morphological characteristics was not studied by many researchers. The present study focuses on the effects of particle size on the shear and interfacial shear behavior of sands through direct shear tests, image analyses and roughness studies. Three different sands of different particle size were selected to study the effect of particle size on the shear and interface shear behavior of these sands. These sands were of same origin and hence the difference in the morphological characteristics of grains was minimal.

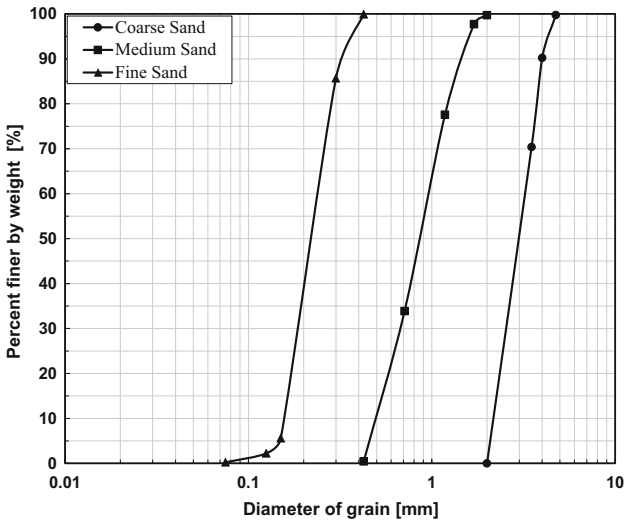

Fig. 1 Grain size of all three sands used in this study

Materials Used in the Study

Sand

Three different types of sands were selected for this study. These sands were obtained by scalping specific size fractions from river sand of same origin. They are coarse sand (CS) (particle size 4.75–2 mm), medium sand (MS) (particle size 2–0.425 mm) and fine sand (FS) (particle size 0.425–0.075 mm), classified as poorly graded sands (SP) as per Unified Soil Classification System. In this paper, these sands as referred as CS, MS and FS. Grain size distribution curves for these sands are presented in Fig. 1. Figure 2 shows the photographs and scanning electron microscopic (SEM) images of sand for understanding the physical appearance and size variations of these sands. Properties of these three different sands are given in Table 1. The median size (D_{50}) of three sands ranged between 3 and 0.22 mm, thus making them suitable for the study to understand the particle size effects on shear behaviour of sand alone and interface behavior of sand–geomembrane.

Geomembrane

A geomembrane made of smooth high-density polyethylene (HDPE) is used in present study. This is the most widely used geomembrane due to its favorable engineering properties like high tensile properties at low strain levels. Properties of geomembrane as given by the manufacturer are listed in Table 2.

Morphological Characteristics of Sand Grains

Morphological characteristics of sand grains represent the overall geometry and shape of the sand grains. Some of

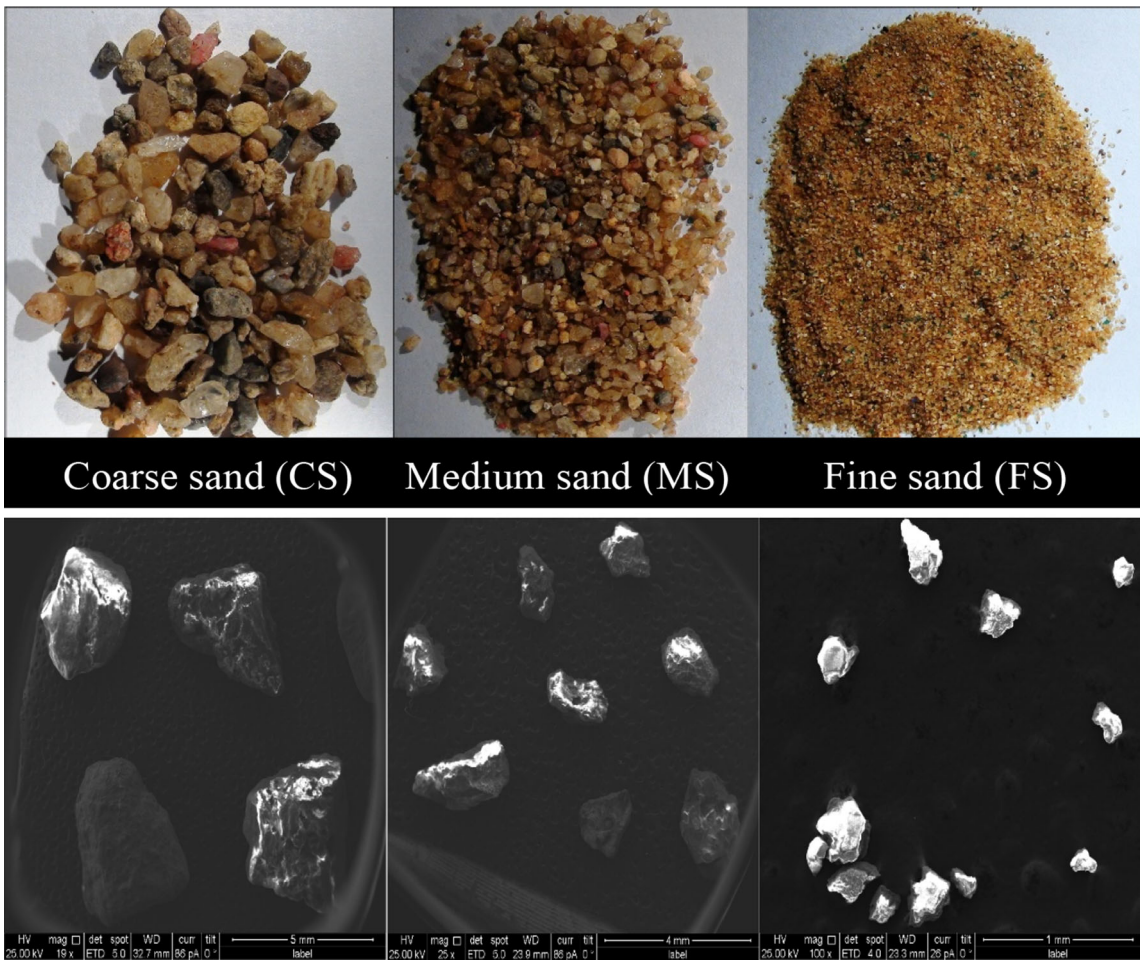

Fig. 2 The photographs and scanning electron microscopic (SEM) images of sand used in study

Table 1 Properties of the sands used in the study

Property Grain size parameters	Coarse sand (CS)	Medium sand (MS)	Fine sand (FS)
D_{10}	2.18	0.50	0.16
D_{30}	2.57	0.68	0.19
D_{50}	3.00	0.87	0.22
D_{60}	3.24	0.97	0.24
Coefficient of uniformity (C_u)	1.49	1.96	1.51
Coefficient of curvature (C_c)	0.93	0.97	0.93
Maximum unit weight (γ_{max}) kN/m^3	15.88	16.09	16.05
Minimum unit weight (γ_{min}) kN/m^3	13.96	13.59	13.10
Maximum void ratio (e_{max})	0.82	0.87	0.95
Maximum void ratio (e_{min})	0.60	0.58	0.60

Table 2 Properties of geomembrane used in the study

Thickness (mm)	Density (g/cm^3)	Tensile strength (N/mm)		Elongation (%)	
		At yield	At break	At yield	At break
1.5	0.942	25	45	12	700

Table 3 Morphological characteristics' descriptors and their formulas along with figures and references are listed here

Descriptor	Formula	Description	Reference
Angularity (A)	$\left(\frac{P_c}{P_e}\right)^2$	Perimeter convex (P_c) is the convex hull perimeter. Perimeter ellipse (P_e) is the perimeter of an equivalent ellipse that has the same area and aspect ratio as the aggregate particle	Pan [22]
Roundness (R)	$\frac{4\pi A}{P^2}$	P is perimeter of any horizontal projected section of the particle at rest A is the area of the profile of the particle projection	Janoo [27]
Sphericity (S)	$\frac{2\sqrt{\pi A}}{P}$	A and P are same as above	Sympatec [30]
Regularity (ρ)	$\frac{(R+S)}{2}$	S = sphericity, R = roundness	Cho et al. [8]
Roughness (R_p)	$\frac{P}{P_c}$	P = perimeter of particle P_c = convex hull perimeter of particle	Janoo [27]
Pictorial representation of notation		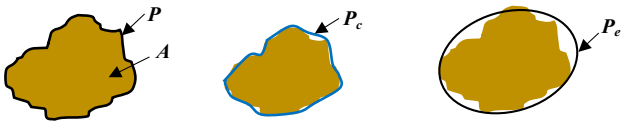	

Table 4 Morphological characteristics of sands

Sand type	Angularity	Roundness	Sphericity	Regularity	Roughness
CS	1.085	0.74	0.86	0.80	1.076
MS	1.091	0.73	0.85	0.79	1.070
FS	1.089	0.74	0.86	0.80	1.065

these parameters selected for this study include angularity, roundness, sphericity and regularity. Definitions of these parameters are given by Pan [22], Pentland [25], Riley [26], Janoo [27], Wadell [28], Krumbein [29] and Sympatec [30]. Physical representation of these parameters along with the formulae used for their calculation are presented in Table 3.

Recent developments in digital vision along with the availability of powerful image processing software has provided the means for the development of an alternate method for soil particle size analysis based on digital image processing. This technology had subsided the ocular based classification and also quantitative judgment made by the individual practicing engineers. In this study the SEM images of 50 particles of each type of sand were taken and used for the determination of their morphological characteristics. This process involves converting the SEM images to binary images and using the pixel information to obtain the geometrical parameters of the grains to calculate the required morphological characteristics as per Table 3. An algorithm was written in MATLAB for the digital image analysis of grains to obtain the morphological characteristics. The morphological characteristics thus determined for all three types of sand are given in Table 4. These parameters were measured from SEM images of sands taken at same magnification. According to the standard particle shape reference charts compiled by Santamarina and Cho [31], all the sands are classified as well rounded. The values of angularity, roundness, sphericity and roughness are nearly same for all the three sands, indicating that the morphological characteristics of these sands are similar.

Direct Shear and Interface Direct Shear Tests

Design of Test Setup

Large size symmetric direct shear test (SDST) setup of sample size (300 mm length × 300 mm breadth × 160 mm height) was used in this study. Description of SDST setup is given in literature [1, 2]. Figure 3 presents the schematic diagram of the modified direct shear test set-up used in the present study. Several modifications were done to the conventional direct shear test set-up for conducting the tests presented in this paper. The upper half of the shear box is completely modified to obtain more uniform stresses and strains along the shear plane during the test as described in earlier studies [1, 2]. The visible front side of the upper half and lower half of the shear box were replaced with a transparent rigid acrylic sheet so as to visualize the particle movement and shear band formation during the tests. The vertical supporting rod for the loading yoke in the conventional direct shear box was replaced by a rectangular

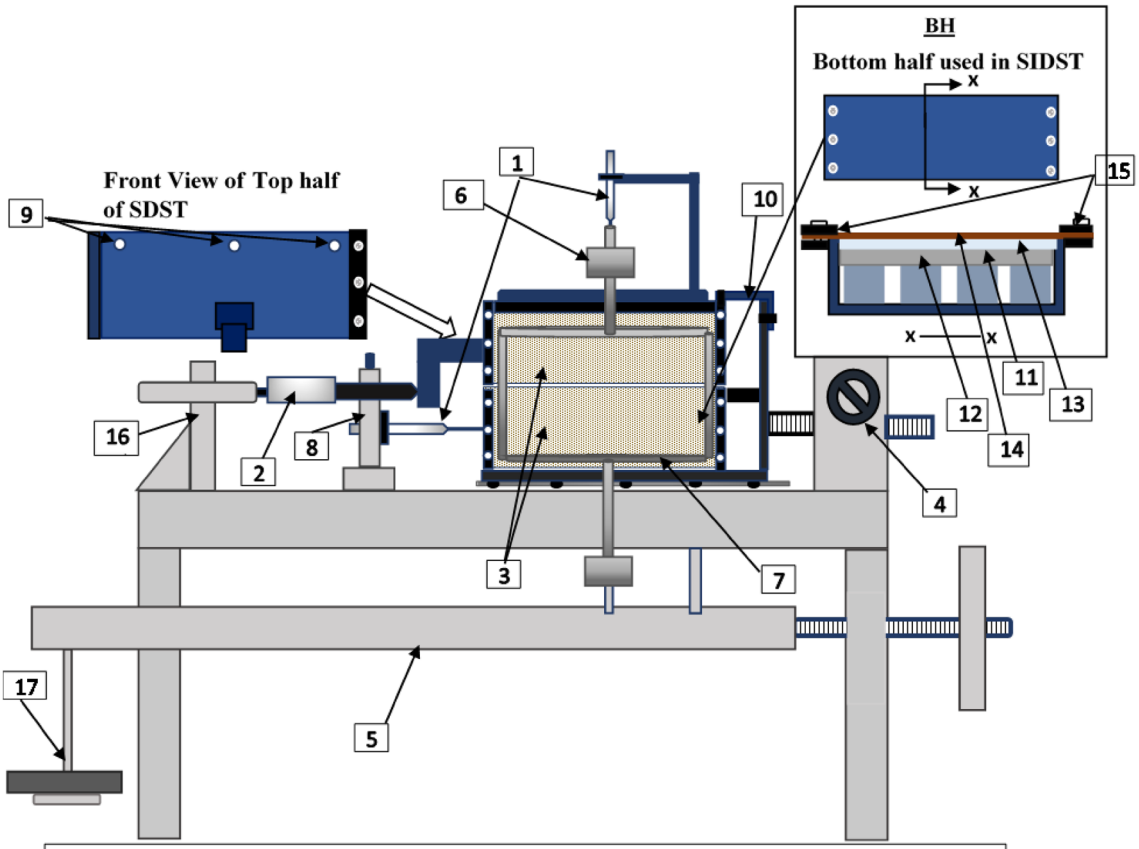

Fig. 3 Schematic diagram of the modified large size direct shear test setup

supporting frame connected to vertical rod to create an obstruction free foreground to the shear box for capturing images and videos (refer part 7 in Fig. 3). This test set-up has a facility to shear the sample up to a larger displacement (75 mm) to understand the post peak behaviour. In interface direct shear tests, the bottom half was replaced with a box consisting of an acrylic sheet attached to a metal sheet, which are supported on rigid concrete blocks (refer to *BH* in Fig. 3). One load cell and two LVDTs were used to measure the shear force and displacements respectively during the test. The setup is integrated with an automatic data acquisition system and graphical display.

Sample Preparation and Testing

Sand was filled in the direct shear box in four layers of equal height. Relative density of sand was maintained as 70 % in all the tests. Weight of the sand required for each layer was calculated and poured into the shear box and was compacted to the predetermined layer thickness. The compaction was carried out by placing a wooden plank of plan size 250 × 250 mm and thickness of 20 mm on the sand sample on which light hammer blows were applied. Number of blows were gradually increased from bottom layer to top layer of the sample to ensure uniform compaction. To study the movement of particles during shear through image analyses, a few vertical colored sand columns were created along the transparent side of the shear box. To fill the colored sand, thin plastic channels of 2 mm thickness and 20 mm width were temporarily attached to the full-height of the transparent side of the shear box at approximately equal spacing to the shear box prior to the filling of sand in the box. Colored sand was filled in these channels through funnel to create colored sand columns up to a height of about 150 mm so as to surpass the shear band thickness. Relative density of the sand is maintained in the colored bands also. After the compaction is complete and the sample is prepared to the full height, the plastic

channels were carefully withdrawn while ensuring that the bands remain intact and distinct from the surrounding sand. In case of interface direct shear tests, bottom half of the shear box was replaced by a rigid base with the provision to fix the geomembrane as explained in the description of test setup. Therefore only upper half of the box was filled with sand in two layers compacted to the required relative density. To avoid the movement the upper half of the shear box during compaction, it was robustly fixed to the platform of the shear box (refer to part 10 in Fig. 3).

After the sample preparation, the load pad is kept on the sample and normal load was applied by a lever arm mechanism. To obtain the symmetric loading conditions in the sample, the load pad was robustly fixed to the shear box with restraining screws available on front and rear sides (refer to part 9 in Fig. 3) of upper half of the shear box. The shear box was then set free by removing the holder restraining the upper half. All the tests were carried out at three normal stresses (σ_n) of 21, 37 and 58 kPa at a displacement rate of 1 mm/min. During the test the evolution of shear band formation in sand alone and sand–geomembrane is visualized and captured through the transparent side using a high definition camera of 12 megapixels.

Results and Discussion

Direct Shear Tests

A series of symmetric loading direct shear tests were conducted on sand. The shear stress–shear displacement responses of the sands under three different normal stresses are presented in Fig. 4. Corresponding volume change responses are presented in Fig. 5. These figures indicate that the stress–strain responses of the sands prior to the peak are almost same for all three sands, irrespective of the large variations in their particle sizes. All the three sands used in the present study have similar morphological characteristics, which is evident from Table 4. Santamarina and Cho [31] and Holtz and Kovacs [32] showed that the stress–strain response of the sands are influenced by the angularity and increasing angularity results in higher peak shear strength due to increase in interlocking forces. The angularity and roundness properties of the sands are almost same in the present study, indicating that the effect of morphology is masked and the variations in the shear behavior are only due to the particle size effects. According to Holtz and Kovacs [32], particle size does not have any effect on the peak friction angle (ϕ_p) if the void ratio is same. For the present samples, void ratios were calculated at 70 % relative density and the same are presented in Table 5. From the table, it is observed that the void ratios of coarse and medium sands are same, whereas the void ratio for FS is slightly higher. Table 1 also presents the range of void ratios for each type of sand. The difference in minimum and maximum void ratios is increasing with the decrease in particle size. However, for 70 % relative density, the difference in the void ratios is not significant, hence the effect of particle size on peak shear strength is negligible.

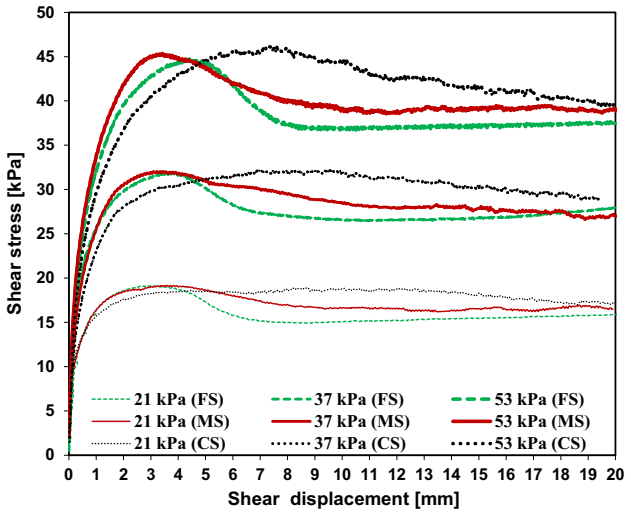

Fig. 4 Shear stress versus shear displacement response of different sands. (Color figure online)

The post-peak stress–strain response of the coarse, medium and FSs is considerably different as observed from Fig. 4. In case of CS, the post peak drop in shear strength is less compared to medium and FSs. FS showed maximum post peak strain softening. The post peak strain softening is increasing with the decrease in particle size, though the relative density of the samples was same in all three cases. Herle and Gudehus [33] and Atkinson [34] showed that the ultimate friction angle (ϕ_r) in direct shear tests is equal to the angle of repose. To confirm this, angle of repose of the coarse, medium and FSs were determined as per ASTM C1444 [35]. In this method, a glass funnel filled with dry sand is held at a specific height to form a sand heap until the funnel is in contact with the heap. This method was used for measuring the angle of repose of sands as well as gravels by several earlier researchers with modifications [36, 37]. Typical measurement of angle of repose for the MS is shown in Fig. 6. After the heap is formed, high definition images were captured in four mutually perpendicular directions and the average angle of repose was estimated. Table 6 gives the values of measured angles of repose for all three types of sands along with their comparison with the ultimate friction angle obtained from direct shear tests. Comparisons showed that the ultimate friction angles were in good agreement with the angles of repose for sands of different grain sizes. Unlike the peak

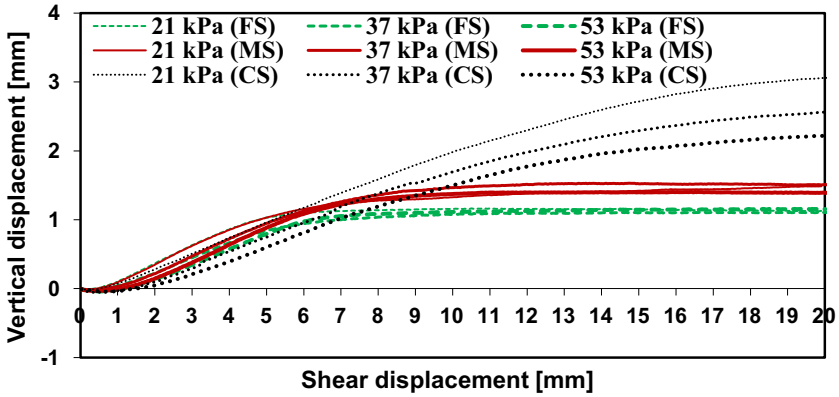

Fig. 5 Vertical displacement versus shear displacement response of different sands. (Color figure online)

Table 5 Void ratios and unit weights of different sands at a relative density of 70 %

Sand	At relative density of 70 %	
	Void ratio (e)	Unit weight (γ) (kN/m^3)
CS	0.67	15.25
MS	0.67	15.26
FS	0.70	15.04

friction angles, the ultimate friction angles were influenced by the size of the particles.

One of the very important aspects of plane strain shearing in sand is the formation of shear bands because they can be related to the failure and strain localization. Well defined shear bands were formed in the direct shear tests with all three types of sands. The shear zone thickness is a significant factor which is correlated with the strain necessary to obtain the failure [38–40]. Thickness of shear bands were determined for the direct shear tests through image segmentation technique explained by Vangla and Latha [2]. Videos of deforming colored sand columns were captured and the images at regular displacement intervals (about 0.1 mm) were extracted and used to find the shear band thickness. Figure 7 shows the deformed (20 mm) and initial (0 mm) profiles of colored sand columns for CS traced and overlapped one over the other so as to see the net deformation and shear band thickness (t) before and after the test. Similar exercise was done for all other sands and it was observed that the thickness of shear bands is increasing with the particle size. Literature [41–43] suggests that the average thickness of the shear zone varies between 5 and 25 times the particle size. It has been also observed that the ratio between shear zone thickness and

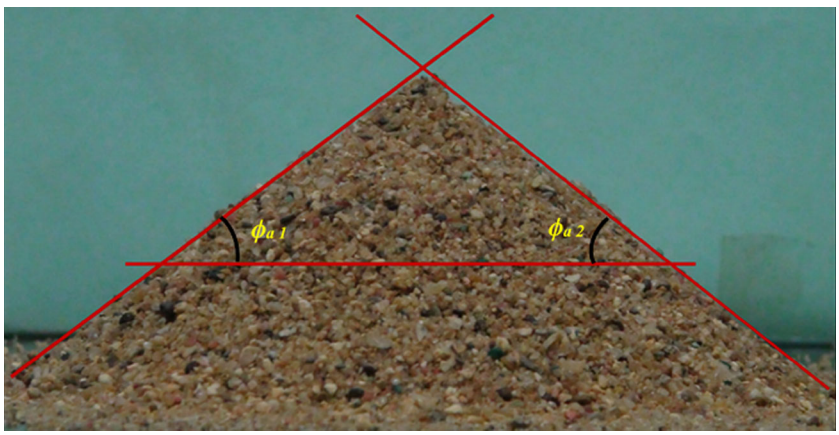

Fig. 6 Determination of angle of repose (ϕ_a) for medium sand

Table 6 Peak friction angle, ultimate friction angle and angle of repose values for different sands

Sand type	Peak friction angle (ϕ_p)	Ultimate friction angle (ϕ_r)	Angle of repose (ϕ_a)
CS	40.8	38.9	37.9
MS	40.7	37.2	36.8
FS	40.4	35.9	35.1

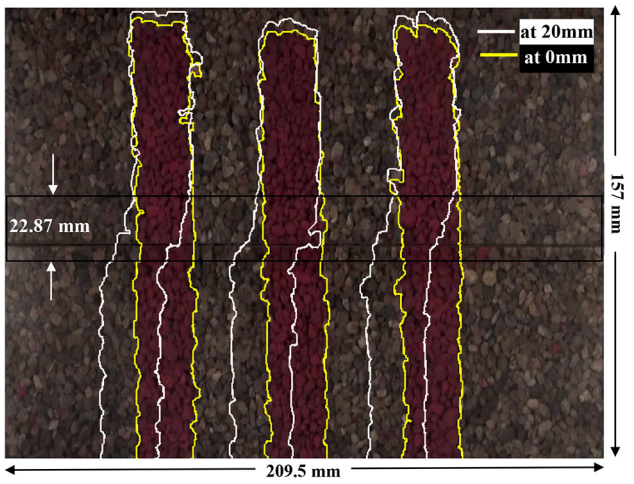

Fig. 7 Estimation of shear band thickness from initial and final profiles of colored sand columns. (Color figure online)

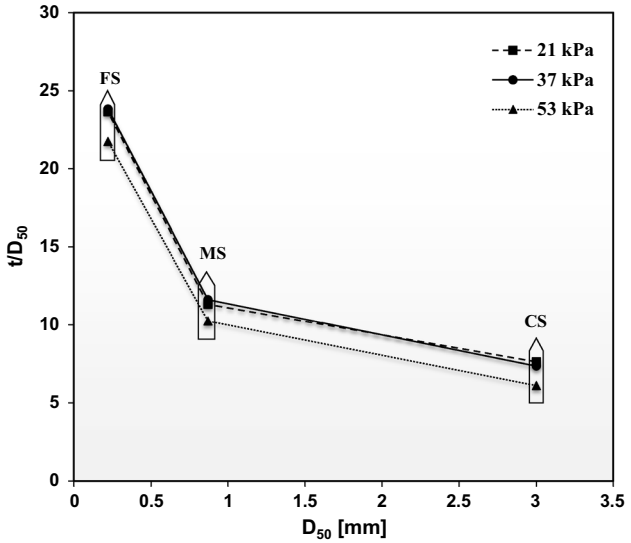

Fig. 8 Variation of normalized shear band thickness with D_{50}

soil particle size depends on the scale of the test (ratio between sample size and particle size), with values considerably larger than 25 having been observed in large scale tests [44]. The shear band thickness measured in the present study is agreeing with these observations. Variation of normalized shear band thickness (t/D_{50}) with the median particle size (D_{50}) is shown in Fig. 8. As observed from Fig. 8, normalized thickness of shear bands is decreasing with the increase in D_{50}, which is in agreement with the observations of earlier researchers [45].

Interface Direct Shear Tests

Interface shear tests were carried out on sand–geomembrane interfaces in SDST setup. All three types of sands

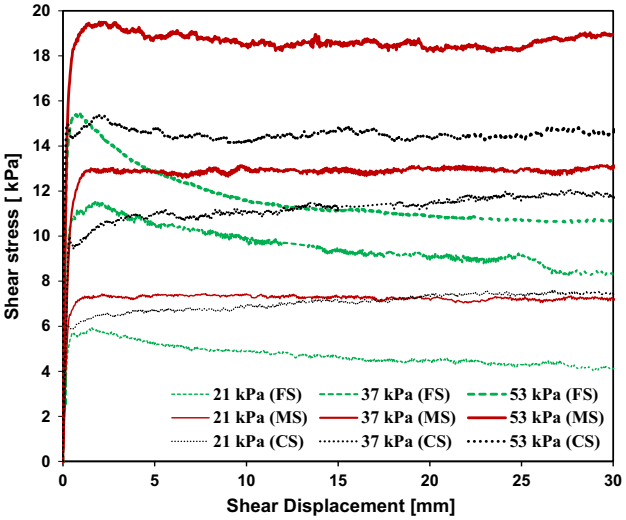

Fig. 9 Shear stress versus shear displacement response of different sands with GM from interface direct shear tests. (Color figure online)

were used in these tests and the tests were carried out under three normal stresses of 21, 37 and 53 kPa. The shear stress-shear displacement responses of the sand–geomembrane interfaces under three different normal stresses are presented in Fig. 9. The shear strength of all the sand–geomembrane interfaces is less than the corresponding sand alone shear strength. As observed from Fig. 9, MS with D_{50} of 0.87 mm is showing highest interfacial frictional resistance with the geomembrane compared to the coarse and fine sands. Also, there is considerable post peak drop in the shear strength in case of FS, unlike coarse and medium sands where the peak strength is sustained for large deformations. Figure 10 presents the comparison on peak and post peak interfacial shear strengths of different sand–geomembrane interfaces, which clearly shows that the drop in peak strength is minimal for coarse and medium sands and significant for FS. The calculated interface friction angle is 0.4 times the ϕ_p for CS, 0.49 times ϕ_p for MS and 0.37 times ϕ_p for FS.

To understand this behavior, microscopic images of geomembrane before and after the test were examined for their surface roughness. Figure 11 presents the microscopic images of geomembrane before the test and the images after the tests for coarse, medium and FSs carried out at 37 kPa. These images clearly show that the CS could make strong impressions leading to plowing and wearing of the surface. Plowing was also evident in case of MS. However, FS could only make lighter impressions on the geomembrane. To quantify the effect of particles on the interfacial friction, both the number of contacts per unit area and the groove depth need to be considered. Groove depth depends on the particle size and angularity as well as the contact stress per particle, which in turn depends on the roughness

and hardness of the particles [17]. In the present study, the roughness and hardness of the sand particles is almost same. The only factor that can influence the interfacial friction in this case is the particle size. A combined effect of number of grooves per unit area and groove depth is realized in the present study. MS showed highest interfacial friction because of increased number of contacts per unit area along with groove depths comparable to CS. In case of CS, though the groove depths are more, number of contacts per unit area were less because of bigger particle sizes. Though the number of contacts per unit area were highest in case of FS, the particles were able to slide along the interface without scarring the surface much as coarse and medium sands do, this can be seen in Fig. 11. Thus the effective number of contacts per unit area (number of particles in contact with the surface and causing grooves of considerable depth in the interfacing material) is the parameter that governs the interfacial shear strength of sands.

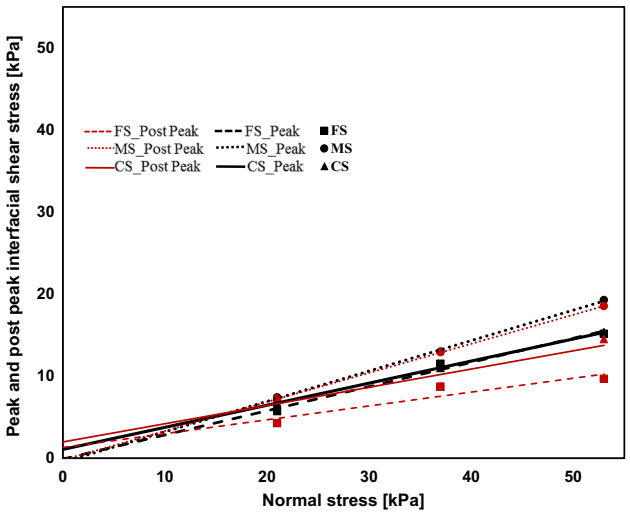

Fig. 10 Peak and post peak interface shear stress versus normal stress from interface direct shear tests. (Color figure online)

Further, surface roughness studies were carried out on the geomembranes before and after the test. A skidless stylus profilometer with maximum traverse length of 50 mm and tip diameter of 2 μm was used for this purpose. The vertical range of this profilometer is 500 μm. Representative specimens of

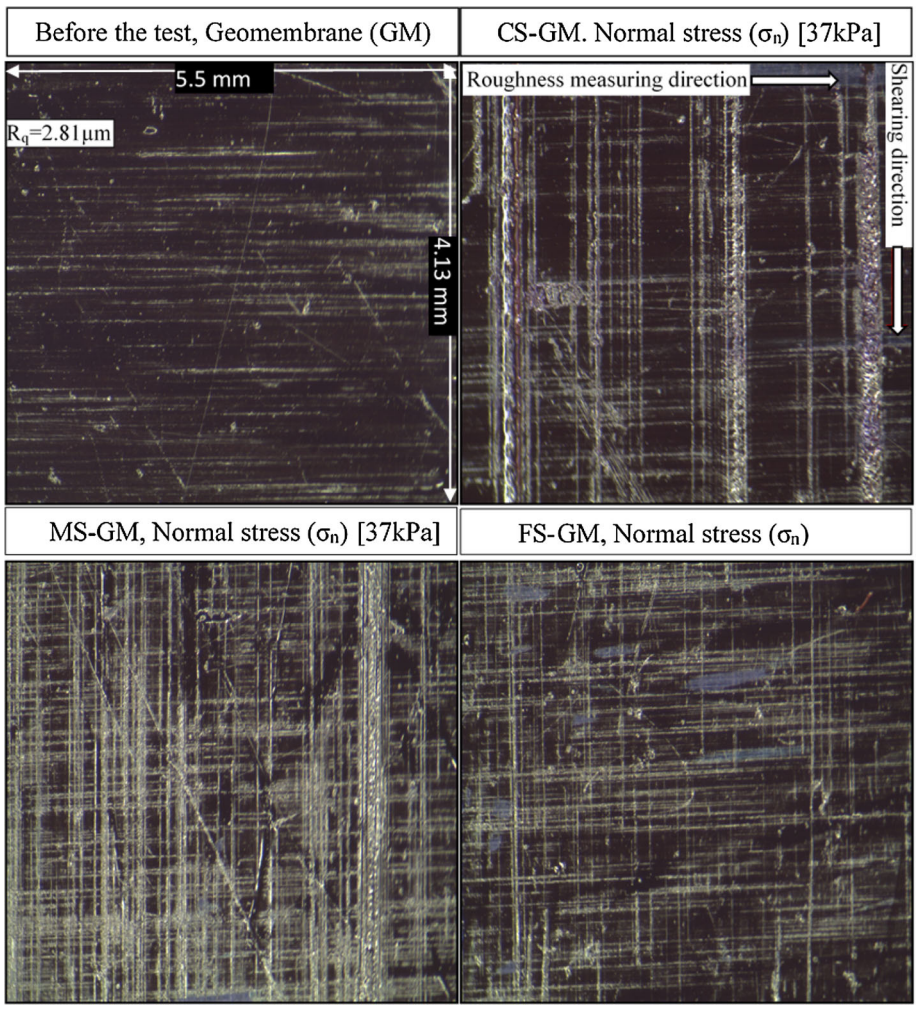

Fig. 11 Microscopic images of geomembrane before and after the interface shear tests with different sands at a normal stress of 37 kPa

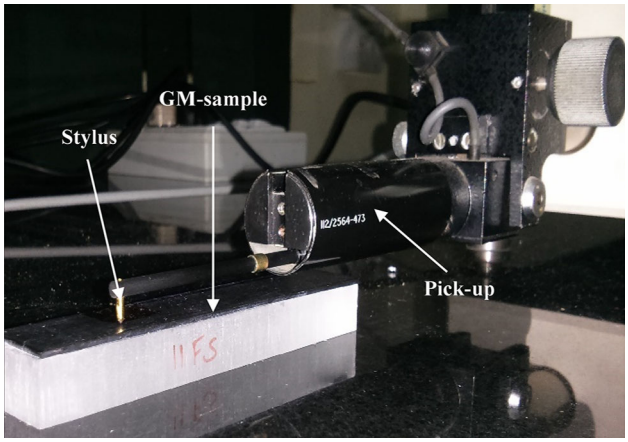

Fig. 12 Stylus profilometer with geomembrane specimen

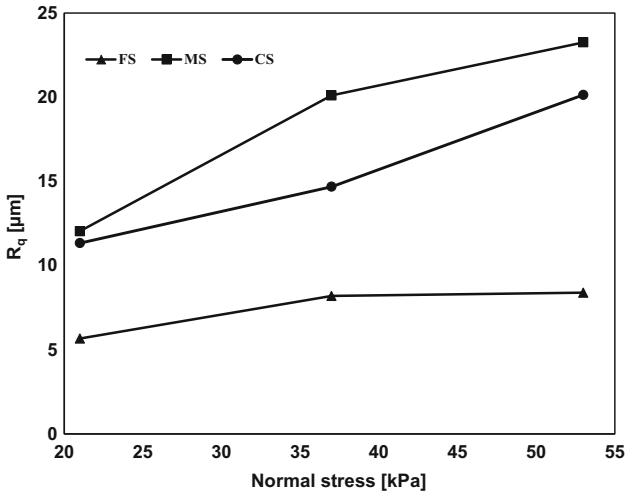

Fig. 13 Variation of R_q for geomembrane after interface tests with sands of different particle size

size 100 × 20 mm were cut from the geomembranes and the surface roughness was determined in the direction perpendicular to the direction of shearing to get the closest estimates of the profile roughness. The measurements were made at four distinct locations for a length of 40 mm in each specimen and the average value was taken. Figure 12 shows the photograph of the stylus profilometer with a specimen in place. Roughness of the specimens is represented by root mean square (RMS) roughness value (R_q), which is defined as the geometric average height of roughness component irregularities from the mean line measured within the sampling length. This value is obtained directly from the measurement using profilometer. Variation of R_q with the normal stress for geomembranes used in interface shear tests with all three types of sands are plotted in Fig. 13. As observed from figure, the surface roughness values increased with the increase in normal stress for all cases because of higher stress applied per unit area. Surface roughness of the geomembrane used in tests with MS was measured to be highest compared to the other two cases because of higher number of contacts per unit area complemented by the particle size, causing grooves of considerable depth. Geomembrane specimen used in the test with FS showed least surface roughness because of the smaller particle size, leading to the sliding of particles without forming deeper grooves. These measurements are in agreement with the visual observations from the microscopic images of these membranes.

Videos captured during the interface shear tests showed that there was no formation of shear bands for sand–geomembrane interfaces because the particles were sliding or being dragged along the interface because the surface of the geomembrane is very smooth. The interface shearing is non-dilative for smooth geomembranes with extremely low vertical deformations as explained in earlier studies of interface shear tests with different geosynthetics [2, 46]. In case of interface shear tests, the governing factor for interfacial shear strength is the relative roughness of the sand and geomembrane which leads to the plowing and formation of grooves rather than the formation of shear bands as observed in sand alone tests.

Conclusions

From the series of direct shear tests on three different sands with different particle sizes and similar morphological characteristics, interface shear tests on these sands with geomembrane and image analysis techniques, the following major conclusions are drawn from the present work.

(1) Peak shear strength of sands with similar morphological characteristics is unaffected by the particle size of sand, when the tests are conducted at same void ratio.
(2) Post peak shear stress response of sands varies with the change in particle size even when the tests are conducted on sands of similar morphology at same void ratio. Ultimate friction angle increases with the particle size, which is confirmed from the angle of repose tests.
(3) Thickness of the shear bands in direct shear tests increases with the increase in particle size. However, the normalized shear band thickness (t/D_{50}) increases with the decrease in particle median size (D_{50}) of sands.
(4) Interface shear strength does not depend on the particle size at a specific void ratio but is influenced by the number of effective contacts per unit area.

Among the three sands tested with geomembrane in interface shear, MS showed higher shearing resistance due to increase in number effective contacts, which is verified through microscopic image analysis and surface roughness studies on the geomembranes before and after the tests.

References

1. Jewell RA (1989) Direct shear tests on sand. Geotechnique 39:309–322
2. Vangla P, Latha GM (2014) Image segmentation technique to analyze deformation profiles in different direct shear tests. Geotech Test J ASTM 37:828–839
3. Mallick SB, Zhai H, Adanur S, Elton DJ (1996) Pullout and direct shear testing of geosynthetic reinforcement: state of art report. Transportation Research Record 1534, Transportation Research Board, National Research Council, Washington DC, 80–90
4. Uesugi M, Kishida H (1986) Influential factors of friction between steel and dry sands. Soils Found 26:33–46
5. Subba Rao KS, Allam MM, Robinson RG (1996) A note on the choice of interfacial friction angle. Geotech Eng ICE Lond 119:123–128
6. Subba Rao KS, Allam MM, Robinson RG (1998) Interfacial friction between sands and solid surfaces. Proc Inst Civ Eng, Geotech Eng 131:75–82
7. Santamarina JC, Cho GC (2004) Soil behavior: the role of particle shape. In: Proceedings skempton conference, London, 1–14
8. Cho G, Dodds J, Santamarina JC (2006) Particle shape effects on packing density, stiffness and strength-natural and crushed sands. J Geotech Geoenviron Eng 132:591–602
9. Göktepe AB, Sezer A (2010) Effect of particle shape on density and permeability of sand. Proc Inst Civ Eng 163:307–320
10. Rouse PC, Fennin RJ, Shuttle DA (2008) Influence of roundness on the void ratio and strength of uniform sand. Geotechnique 58:227–231
11. Shinohara K, Mikihiro O, Goldman B (2000) Effect of particle shape on angle of internal friction by triaxial compression test. Powder Technol 107:131–136
12. Witt KJ, Brauns J (1983) Permeability- anisotropy due to particle shape. J Geotech Eng 109:1181–1187
13. Williams ND, Houlihan MF (1987) Evaluation of interface friction properties between geosynthetics and soils. In: Proceedings of geosynthetics 87, New Oreleans, 616–627
14. Fuggle AR, Frost JD (2010) Particle size effects in interface shear behavior and geomembrane wear. In: Proceedings of international symposium on characterization and behavior of interfaces, IOS, Atlanta, pp. 51–57
15. O'Rourke TD, Druschel SJ, Netravali AN (1990) Shear strength characteristics of sand polymer interfaces. J Geotech Eng 116:451–469
16. Dove JE (1996) Particle-geomembrane interface strength behavior as influenced by surface topography, Ph.D. Dissertation, School of Civil and Environmental Engineering, Georgia Institute of Technology, Atlanta
17. Dove JE, Frost JD (1999) Peak friction behavior of smooth geomembrane particle interfaces. J Geotech Geoenviron Eng 125:544–555
18. Athanasopoulos GA (1993) Effect of particle size on the mechanical behaviour of sand-geotextile composites. Geotext Geomembr 12:255–273
19. Lim MS, Wijeyesekera DC, Zainorabidin A, Bakar I (2012) The effects of particle morphology (shape and sizes) characteristics on its engineering behaviour and sustainable engineering performance of sand. Int J Integr Eng 4:27–37
20. Santamarina JC, Cascante G (1998) Effect of surface roughness on wave propagation parameters. Geotechnique 48:129–137
21. Fuggle AR (2011) Geomaterial gradation influences on interface shear behavior. Ph.D. Dissertation, School of Civil and Environmental Engineering, Georgia Institute of Technology, Atlanta
22. Pan T (2002) Fine aggregate characterization using digital image analysis. Master's Thesis, Louisiana State University, USA
23. Altuhafi F, O'Sullivan C, Cavarretta I (2013) Analysis of an image-based method to quantify the size and shape of sand particles. ASCE J Geotech Geoenviron Eng 139:1290–1307
24. Ohm HS (2013) Image-based soil particle size and shape characterization. PhD Thesis, University of Michigan, Ann Arbor, MI
25. Pentland A (1927) A method of measuring the angularity of sands. MAG MN AL Acta Eng Dom 21:XCIII
26. Riley NA (1941) Projection sphericity. J Sediment Petrol 11:94–97
27. Janoo V (1998) Quantification of shape, angularity and surface texture of base coarse materials. Cold Regions Research and Engineering Laboratory, US Army Corps of Engineers, Vermont Agency of Transportation, Special Report 98–101
28. Wadell H (1935) Volume, shape and roundness of quartz particles. J Geol 43:250–279
29. Krumbein WC (1941) Measurement and geological significance of shape and roundness of sedimentary particles. J Sediment Petrol 11:64–72
30. Sympatec (2008) Germany windox 5.4.1.0—operating instructions. 475–476
31. Santamarina JC, Cho GC (2001) Determination of critical state parameters in sandy soils—simple procedure. Geotech Test J 24:185–192
32. Holtz RD, Kovacs WD (1981) An introduction to geotechnical engineering. Prentice-Hall, Inc. Englewood cliffs
33. Herle I, Gudehus G (1999) Determination of parameters of a hypoplastic constitutive model from properties of grain assemblies. Mech Cohesive-Frict Mater 4:461–486
34. Atkinson J (2007) The mechanics of soils and foundations. Taylor and Francis, London
35. ASTM C1444-00 (2001) Standard method for measuring the angle of repose of free-flowing mold powders. In: Annual Book of ASTM Standards, American Society of Testing and Materials, Philadelphia, p 694–695
36. Miura K, Maeda K, Toki S (1997) Method of measurement for the angle of repose of sands. Soils Found 37:89–96
37. Zhichao Liu (2008) Measuring the angle of repose of granular systems using hollow cylinders, Master of Science Thesis, B S Southwest Jiaotong University, China
38. Cerato AB, Lutenegger AL (2006) Specimen size and scale effects of direct shear box tests of sands. Geotech Test J 29:1–10
39. DeJaeger J (1994) Influence of grain size and shape on the dry sand shear behaviour. In: Proceedings of the 13th international conference on soil mechanics and foundation engineering 1:13–16
40. Kita K, Okamura M (2000) Bearing capacity test. Centrifuge 98(2):1067–1075
41. Roscoe KH (1970) Tenth Rankine lecture: the influence of strains in soil mechanics. Geotechnique 20:129–170
42. Hartley S (1982) Shear bands in sand part II. Project Report, Department of Engineering, University of Cambridge, UK
43. DeJaeger J (1991) Influence de la morphologie des sables sur leur comportement mecanique. Ph.D. Thesis, Université Catholique de Louvain, Louvain-la-Neuve
44. Palmeira EM, Milligan GWE (1989) Scale effects in direct shear tests on sand. In: Proceedings of the 12th international conference

on soil mechanics and foundation engineering, Rio de Janeiro, Brazil, 1:739–742
45. Alshibli KA, Sture S (1999) Sand shear band thickness measurements by digital imaging techniques. J Comput Civil Eng 13:103–109
46. Dove JE, Bents DD, Wang J, Gao B (2006) Particle-scale surface interactions of non-dilative interface systems. Geotext Geomembr 24:156–168